Audio Engineering Society
Convention Paper

Presented at the 139th Convention
2015 October 29–November 1 New York, USA

This paper was peer-reviewed as a complete manuscript for presentation at this Convention. This paper is available in the AES E-Library, http://www.aes.org/e-lib. All rights reserved. Reproduction of this paper, or any portion thereof, is not permitted without direct permission from the Journal of the Audio Engineering Society.

Time/Phase Behavior of Constant Beamwidth Transducer (CBT) Circular-Arc Loudspeaker Line Arrays

D. B. (Don) Keele, Jr.[1]

[1] DBK Associates and Labs
Bloomington, IN, 47408 USA
DKeeleJr@Comcast.net

ABSTRACT

This paper explores the time and phase response of circular-arc CBT arrays through simulation and measurement. Although the impulse response of the CBT array is spread out in time, it's phase response is found to be minimum phase at all locations in front of the array: up-down, side-to-side, and near-far. When the magnitude response is equalized flat with a minimum-phase filter, the resultant phase is substantially linear phase over a broad frequency range at all these diverse locations. This means that the CBT array is essentially time aligned and linear phase and as a result will accurately reproduce square waves anywhere within its coverage. Accurate reproduction of square waves is not necessarily audible but many people believe that it is an important loudspeaker characteristic. The CBT array essentially forms a virtual point-source but with the extremely-uniform broadband directional coverage of the CBT array itself. When the CBT array is implemented with discrete sources, the impulse response mimics a FIR filter but with non-linear sample spacing and with a shape that looks like a roller coaster track viewed laterally. An analysis of the constant-phase wave fronts generated by a CBT array reveals that the sound waves essentially radiate from a point that is located at the center of curvature of the array's circular arc and are essentially circular at all distances, mimicking a point source.

1. INTRODUCTION

One aspect of constant beamwidth transducer CBT loudspeaker arrays that has not been investigated is its time and phase behavior. Previous work has shown that CBT surface and line arrays [3 - 10] have extremely-uniform broad-band coverage, constant beamwidth, and directivity behavior but this prior work considered only the magnitude response of the radiated sound field and completely neglected the time and phase behavior of the array's acoustic radiation.

This paper explores in detail via simulation and measurement the time and phase performance of CBT arrays. Although primarily covering just circular-arc CBT arrays, the work applies equally well to straight-line and flat-panel delay-curved CBT arrays [3, 4].

The paper shows that the phase response of a properly implemented CBT array is effectively minimum phase

at all locations in its coverage region and furthermore is essentially identical at all these locations once the transport delay between the array and the pressure sample location is accounted for.

This minimum-phase condition at all coverage locations implies that the phase response can be turned into a linear-phase condition by applying minimum phase compensation to flatten the magnitude response. Subsequently, the flat magnitude and phase response implies that the system will properly reproduce square waves at all these same diverse locations.

The time response of a CBT array, although composed of numerous separate individual contributions from all the sources of the array, exhibits a uniform comb-free response as long as the center-to-center spacing of the array's sources is less than about a half wavelength at the highest operating frequency of the array.

The paper shows that the 3D radiation of a CBT array is essentially that of a point source but with the controlled radiation pattern of the CBT array itself. Sound-field simulations show that the effective center of curvature of the constant-phase wave fronts is located at the array's center of curvature.

1.1. A Brief CBT History

Constant beamwidth transducer CBT array theory is based on un-classified military under-water transducer research done in the late 1970s and early 80s [1, 2]. The research describes a curved-surface transducer in the form of a spherical cap with frequency-independent Legendre shading that provides wide-band extremely-constant beamwidth, coverage, and directivity behavior with virtually no side lobes. The theory was applied to loudspeaker arrays by Keele in 2000 [3] where he extended the concept to circular-arc line arrays and further explored the CBT concepts in a series of seven additional AES papers between 2002 and 2015 [4 - 10].

A CBT circular-arc line array is quite simple and straight forward to implement. No complicated DSP processing is required. Just arrange the speakers around a circular arc and apply simple frequency-independent amplitude-only Legendre shading [3, Eq. 3, page 6]. This forms an array that exhibits broad-band constant-directivity and beamwidth behavior with extremely even coverage at all points from near-to-far, up and down, and side to side. Analysis shows that the CBT array essentially has no complex near field. Its near-field coverage is basically equal to its far-field coverage.

2. ENGLISH OR METRIC DIMENSIONS?

The author apologizes for the mixed use of both English and metric dimensions in this paper. All the simulators used in this paper were originally programmed using English dimensions and the author has not taken the time to modify the programs.

3. SIMULATED ARRAY DESCRIPTION AND FAR FIELD PERFORMANCE

This section describes the array configuration that was chosen for the simulations and presents some simulations of its far-field beamwidth and power rolloff behavior.

3.1. Physical Description

The simulated array is a free-standing 180° circular-arc array. The array height and depth is 40" and is composed of 112 point sources spaced at about 0.56" (14.2 mm). The array is shaded with full continuous Legendre shading that is not truncated or stepped [6].

The 180° array configuration was chosen to essentially mimic the array that was available for the experimental measurements [see Section 9 Fig. 32 later in this paper].

The following figure shows the side, front, and top views of the simulated array. The line width (red) is proportional to the shading of the array, i.e. the front of the array is at maximum (broad line) and tapers down towards the top and bottom ends of the array (narrow line).

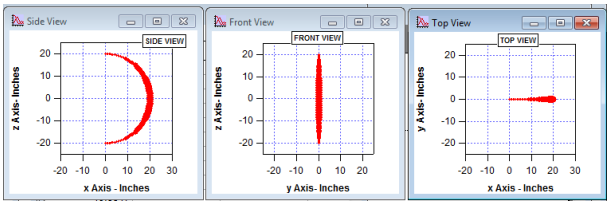

Fig. 1. Side, front, and top views of the 180° circular-arc array used to generate all the simulations used in this paper. The array is 40" tall. The red line width indicates the strength of the array's Legendre shading.

3.2. Beamwidth

The simulated far-field beamwidth (- 6dB) is shown in the following figure. The simulation predicts that the beamwidth is very constant and is held at approximately 115° held over a very broad range from about 250 Hz to 20 kHz.

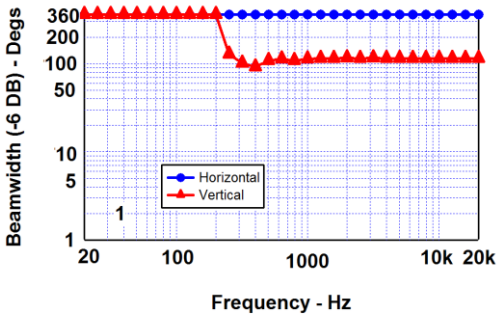

Fig. 2. The predicted beamwidth (-6 dB) of the simulated array of Fig. 1. The 115° beamwidth is maintained down to about 250 Hz. Note the extreme uniformity of the beamwidth over the whole frequency range.

3.3. Power Roll Off

The simulated on-axis power rolloff of the array is shown in the following figure. The power rolloff compares the actual simulated on-axis response to the level that would exist if all the sources were in phase at the sample location. This roll off is exhibited at all points in the coverage of the array both on- and off-axis, and in its power response and must be compensated with equalization.

A circular-arc array exhibits a power rolloff of about -3 dB/octave (-10 dB/decade) above a certain frequency that depends on the height and angle of the array.

The next figure shows the on-axis power rolloff of the simulated array. The power rolls off smoothly above 300 Hz.

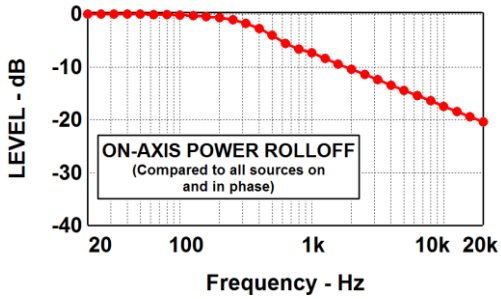

Fig. 3. The predicted power rolloff of the simulated array of Fig. 1. Above 250 Hz the response rolls off very smoothly at 3 dB/octave (10 dB/decade).

4. IMPULSE RESPONSE OF STRAIGHT-LINE AND CIRCULAR-ARC CBT LINE ARRAYS

This section investigates the impulse response of two different types of line arrays: 1) a 56-point 40”-tall straight-line equally-driven array and 2) a 56-point circular-arc 40”-tall CBT array with full continuous Legendre shading. The impulse response is not simulated in the far field but at points close to the array essentially in the near field.

4.1. Simulation Conditions

The impulse response for both arrays was calculated at four vertical off-axis angles of 0°, 15°, 30°, and 45° with rotation around the front center of the arrays at a fairly close distance of 80” (about 2 m).

The following figure shows the location of the sample points in relation to both arrays.

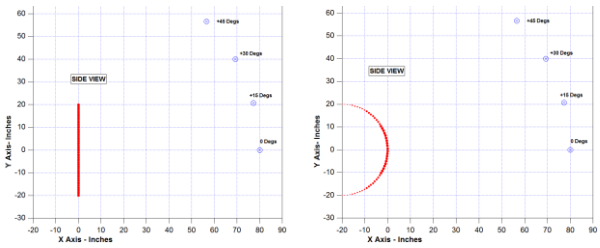

Fig. 4. Impulse response sample locations for both the straight line (left) and circular-arc CBT arrays (right). The locations are arranged around an 80” radius circle at angles of 0°, 15°, 30°, and 45°. Rotation is about the front center of each array.

4.2. Graphical Display

The impulse response as defined here is not the conventional continuous impulse response as a function of time but a response that shows the individual arrival amplitudes and times in a stick-figure display.

In other words, the impulse response is displayed as amplitude vs. time in a sticks-to-zero display with dots on top showing the location and strength of each individual signal generated by each source in the array.

4.3. Straight-Line Array with Equal Shading

The impulse response of the 56-point 40" tall straight-line equally driven array is shown in the next four figures at each of the off-axis angles. Note that the impulse response in each case is essentially rectangular in shape with a slight downward tilt with time.

Note also that the width of the impulse package widens as the angle increases. This is because as the observation angle increases, the points on the top of the array are closer to the observation point while equivalently the points on the bottom of the array get farther away.

The impulse response forms a type of FIR (finite impulse response) filter but with non-linear spacing of the samples. This FIR filter essentially filters the spatial output of the array at the different angles. It is the rectangular nature of the straight-line array's impulse response that contributes to its poor polar coverage, i.e. no tapering or shading.

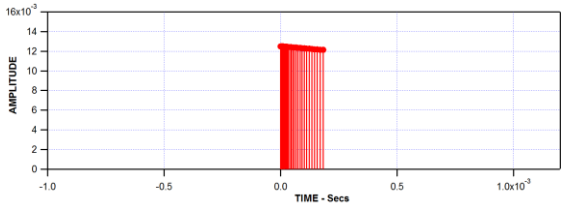

Fig. 5. Time response for the 40"-tall straight line array at an on-axis angle of 0°. See Fig. 4 for conditions. Note the compact nature of the impulse response in time.

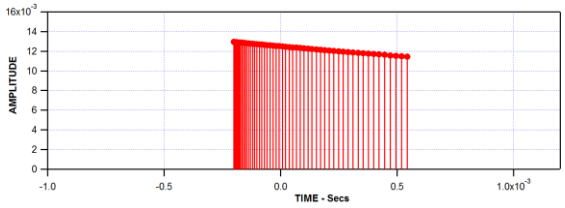

Fig. 6. Time response for the 40"-tall straight line array at an angle of 15°. See Fig. 4 for conditions.

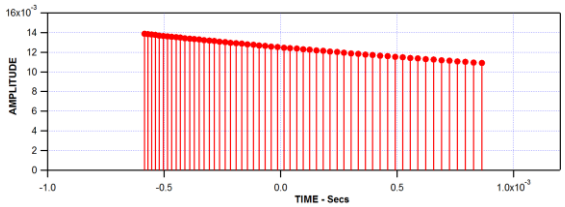

Fig. 7. Time response for the 40"-tall straight line array at an angle of 30°. See Fig. 4 for conditions.

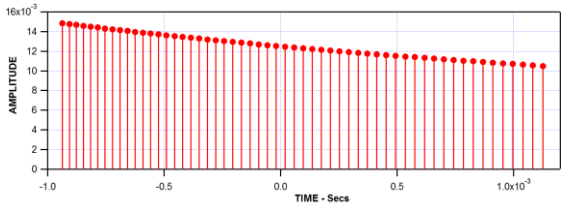

Fig. 8. Time response for the 40"-tall straight line array at an angle of 45°. See Fig. 4 for conditions. Note how the impulse response is spread out in time at this off-axis angle.

4.4. CBT Circular-Arc Array with Full Legendre Shading

The impulse response of the CBT circular-arc line array is shown in the next four figures at each off-axis angle. Note that the impulse response in each case exhibits the Legendre shading by a strong tapering of the impulse from maximum at low times to minimum at high times. Each impulse response exhibits a very distinctive shape that resembles a single summit of a roller coaster track when viewed from different lateral angles.

The tapering of the CBT array's impulse response is the primary reason that array exhibits excellent polar response.

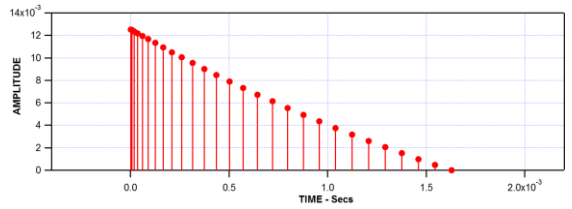

Fig. 9. Time response for the 40”-tall CBT array at an angle of 0°. See Fig. 4 for conditions.

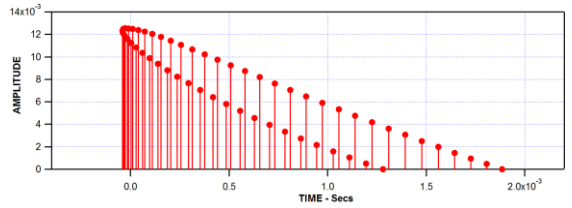

Fig. 10. Time response for the 40” tall CBT array at an angle of 15°. See Fig. 4 for conditions.

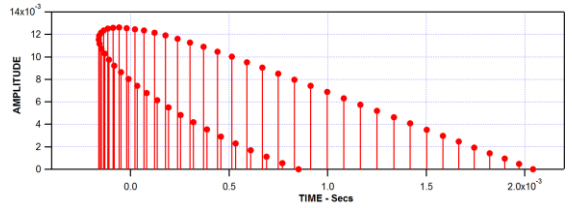

Fig. 11. Time response for the 40” tall CBT array at an angle of 30°. See Fig. 4 for conditions.

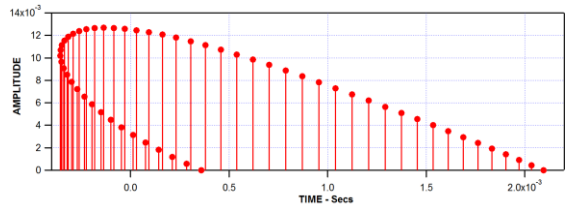

Fig. 12, Time response for the 40” tall CBT array at an angle of 45°. See Fig. 4 for conditions.

5. FAR-FIELD CBT MAGNITUDE/PHASE RESPONSE AND POWER ROLLOFF

The next three figures illustrate the far-field magnitude and phase behavior of the CBT array of Fig. 1 at a simulated distance of 1,000” (83.3 ft or about 25 m). The simulations were run at three locations: 1) on axis, 2) 45° off-axis vertical, and 3) 45° off-axis horizontal. Center of rotation in every case was at the front of the array.

Two situations at each location were simulated: 1) a raw response without equalization, and 2) an equalized response. NOTE: *In case 2), the magnitude/phase equalization point was not in the far field but in the near field of the array at a very-close on-axis distance of 20”.*

Although the CBT line array’s raw magnitude frequency response exhibits a 3 dB/octave power rolloff above a frequency governed by the size of the array and its coverage angle [3], this rolled-off magnitude and resultant phase frequency response remains essentially the same at all locations within the defined coverage of the CBT array due to the CBT arrays extremely even broadband coverage.

5.1. Far-Field Coverage Data

The following three figures illustrate the magnitude/phase data for the CBT array of Fig. 1. In each figure the raw un-equalized data is on the left and the equalized data is on the right. Note that the un-equalized magnitude data has been normalized to 0 dB at 100 Hz to compensate for far-field level drop off.

5.1.1. On Axis

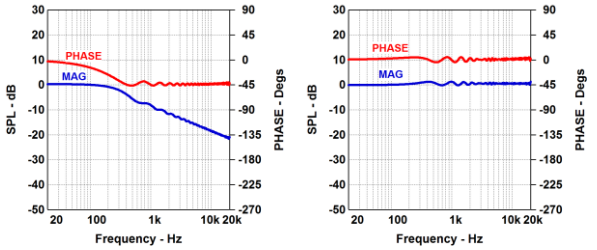

Fig. 13. Magnitude/phase data on-axis (0°) at 25 m. Un-equalized (left) and equalized (Right).

5.1.2. Vertical at 45° Up

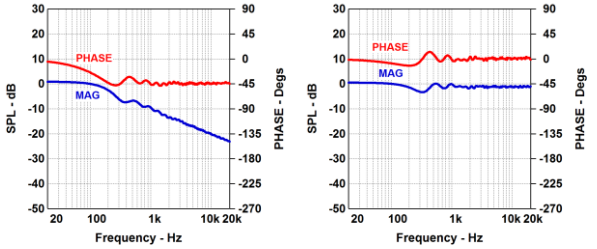

Fig. 14. Magnitude/phase data off-axis vertically (45°) at 25 m. Un-equalized (left) and equalized (Right).

5.1.3. Horizontal at 45° to the Side

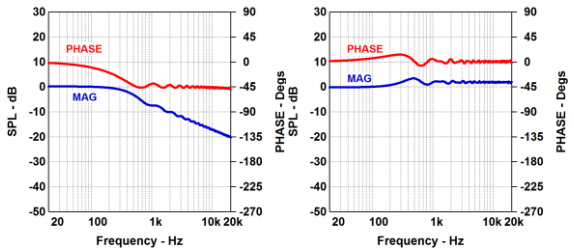

Fig. 15. Magnitude/phase data off-axis horizontally (45°) at 25 m. Un-equalized (left) and equalized (Right).

5.2. Far-Field Data Observations

At each far-field location, note how similar the raw and equalized magnitude and phase responses are to each other. Note that the magnitude responses in each un-equalized (raw) graph (left graphs in each figure) all exhibit the same rolled-off power response characteristic pointed out in the "Power Roll Off" section. This means that if the power roll off is equalized flat at one location, it will also be flat at all the other locations!

6. CBT SOUND-FIELD ANALYSIS

This section illustrates the vertical magnitude and phase sound fields of the 40"-tall CBT array of Fig. 1 at octave-spaced frequencies in the range of 250 Hz to 4 kHz.

The left display in each pair of graphs shows the magnitude sound field. The array location is clearly shown on the left by the bright yellow coloration. Even the array's Legendre shading is clearly indicated.

The right grey-scale display in each pair of graphs shows the phase sound field with phase rotations clearly shown as distance increases from the array. Each phase contour represents the shape of the constant-phase wave front.

Note that the distance between the major phase transitions represents exactly one wavelength. This distance decreases as frequency increases to illustrate how the wavelength decreases as frequency increases.

Note also that the shapes of the constant-phase contours are essentially circular at all analyzed frequencies with the center of curvature located roughly at the center of curvature of the circular array.

6.1. Magnitude and Phase Wave Front Displays

The following five figures show the magnitude (left) and phase (right) sound fields at frequencies of 250 Hz, 500 Hz, 1 kHz, 2 kHz, and 4 kHz for the array of Fig. 1. In each case, the sound field is shown in a 120" x 120" (roughly 3 m x 3 m) region with the array centered vertically on the left of the region.

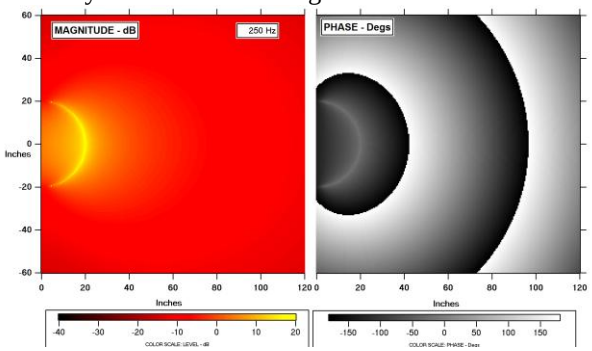

Fig. 16. CBT array sound field at 250 Hz.

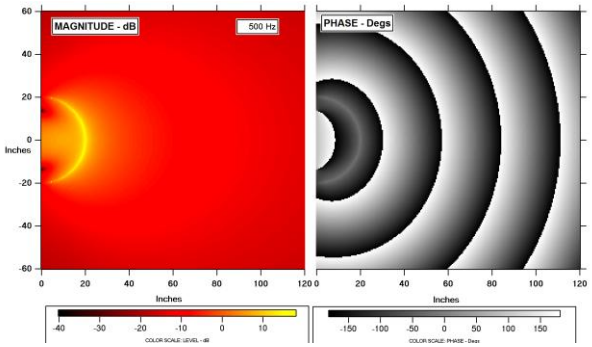

Fig. 17. CBT array sound field at 500 Hz.

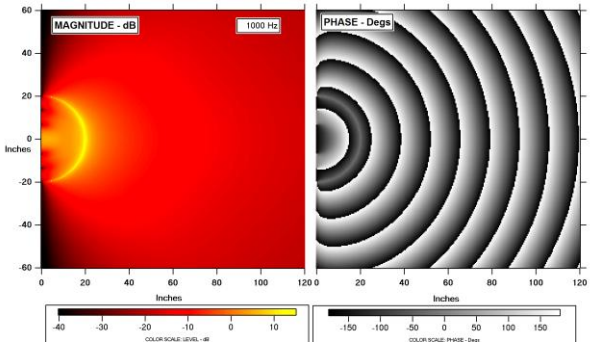

Fig. 18. CBT array sound field at 1 kHz.

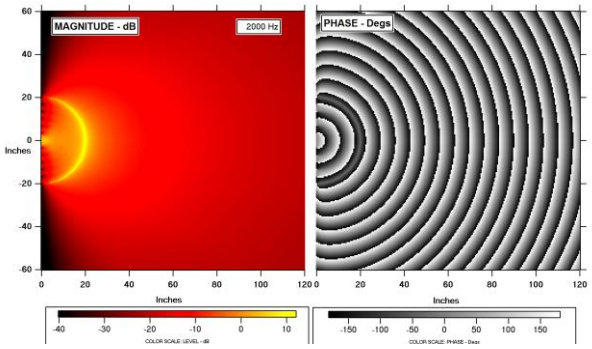

Fig. 19. CBT array sound field at 2 kHz.

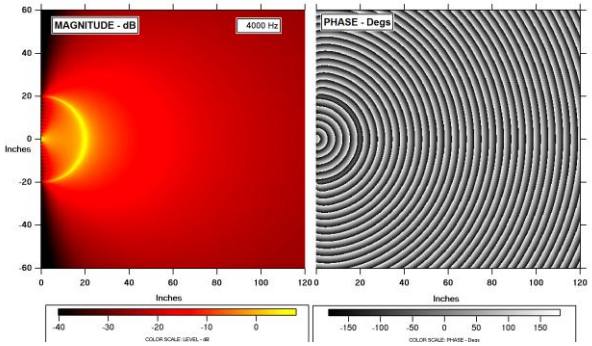

Fig. 20. CBT array sound field at 4 kHz.

6.2. Sound-Field Observations

These displays show the extremely-uniform sound fields radiated by the CBT array. The very-consistent sound-field behavior of the CBT array means that the array essentially radiates as a virtual point source but with the directional characteristics of the CBT array itself. The constant-phase wave fronts show that the sound waves essentially radiate from a point that is located at the center of curvature of the array's circular arc.

7. CBT ARRAY NEAR FIELD MAGNITUDE AND PHASE RESPONSE VARIATION WITH HEIGHT AND ANGLE

This section illustrates how the magnitude and phase response of the CBT array of Fig. 1 changes at different locations close to the array which are essentially in the array's near field. Responses at off-axis locations vertically and horizontally in front of and to the sides of the array are shown.

As before, the simulations show that all the predicted data is extremely uniform and consistent at all the analyzed locations.

7.1. Vary Height

A rising straight-line trajectory in front of the array at a distance of 20" was chosen to illustrate how the response changes with height. Individual magnitude and phase responses were calculated at six heights ranging from 0 to 50" with a distance increment of 10".

As in Section 5, pairs of data graphs were calculated at each location to show the raw un-equalized (left) and equalized (right) responses. NOTE: *As before, the response was magnitude/phase equalized flat not at a point in the far field, but at a very close on-axis point in the near field of the array at a distance of 20".*

7.1.1. Height Locations

The following figure shows the location of each response calculation point on a vertical line in front of the array. The heights span a vertical range of 50" with increments of 10" at a distance of 20" in front of the array.

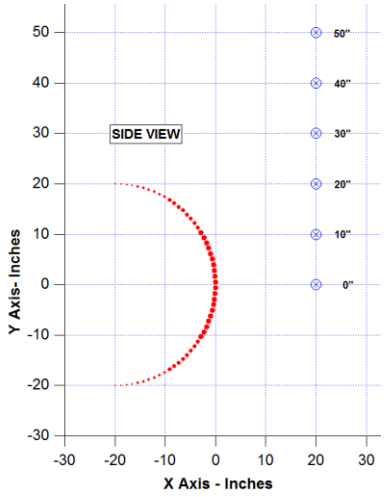

Fig. 21. Array side view with height calculation locations in front of the array at a distance of 20". The points were equally distributed along a straight line rising from 0" to 50" in steps of 10".

7.1.2. Response with Height

The following three figures show the magnitude/phase results at each of the different heights.

The first two figures show pairs of representative magnitude/phase responses at two heights of 0" and +20" and a distance of 20" from the front of the array.

The last figure of the three shows a pair of graphs that illustrate all the heights magnitude/phase responses overlaid in one plot with the un-equalized set on the left and the equalized set on the right.

As before, the equalization point was on axis at 20". This corresponds to the lowest point of the analyzed range of heights.

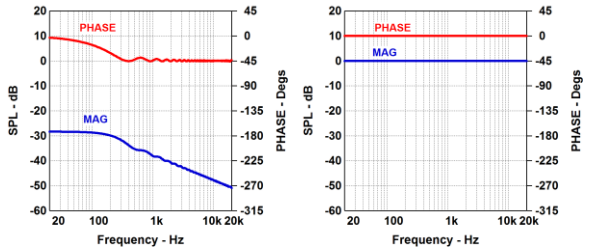

Fig. 22. Magnitude/phase data on axis (height = 0"). Un-equalized (left) and equalized (right). Note that this is the equalized location and thus the responses shown on the right are straight lines.

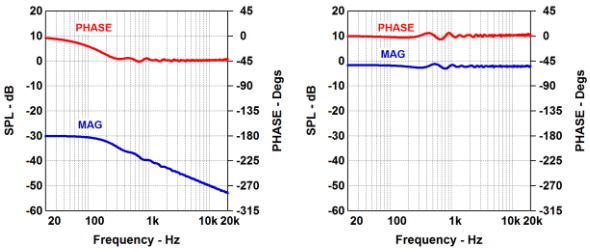

Fig. 23. Magnitude/phase data at a height of 20". Un-equalized (left) and equalized (right).

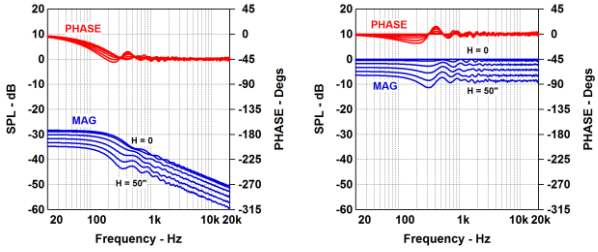

Fig. 24. Magnitude/phase data at various heights from 0 to 50" with steps of 10". Un-equalized (left) and equalized (right). Note the uniformity of the curves. The magnitude response levels decrease with height because the array is farther away.

7.1.3. Variation with Height Observations

The overlaid magnitude/phase responses shown in the last graph of the three illustrate the extreme uniformity of the curves with height. The only aberrations exhibited are response variations in the low end of the array's operating range from 200 Hz to 1 kHz.

7.2. Vary Angle

A circular 90° trajectory around the front of the array of Fig. 1 at a distance of 20" was chosen to illustrate how the response changes with horizontal angle. Individual magnitude and phase responses were calculated at four angles ranging from 0 to 90° with an angle increment of 30°.

7.2.1. Angle Locations

The next figure shows the location of each response calculation point. The data calculated at these locations illustrates how the magnitude/phase response changes with horizontal off-axis angle. The angles cover a circular range of 90° from on axis to 90° off axis with increments of 30° at a distance of 20" in front of the array.

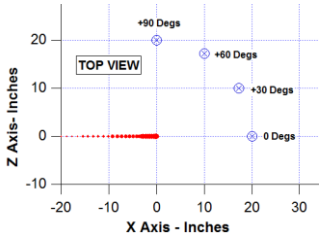

Fig. 25. Array top view with horizontal off-axis angle calculation locations in front of the array at a radius of 20". Off-axis angles of 0°, 30°, 60°, and 90° are indicated.

7.2.2. Response vs. Angle

The following figure shows a composite of the magnitude/phase results at each of the different angles.

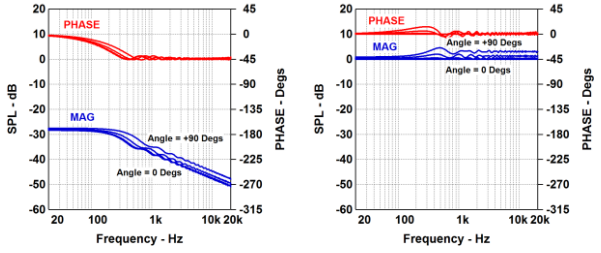

Fig. 26. Magnitude/phase data at various off-axis horizontal angles from 0° to 90° with steps of 30°.

7.2.3. Variation with Angle Observations

The overlaid magnitude/phase off-axis horizontal responses shown in the last figure show the extreme uniformity of the curves with angle. As with the height curves, the only aberrations exhibited are response variations in the low end of the array's operating range from 200 Hz to 1 kHz. The magnitude response levels actually increase somewhat as the horizontal angle increases because the array's sources become more and more equidistance from the sample location

8. COMB FILTERING QUESTIONS

One aspect of the CBTs impulse response that I investigated is related to a question that someone asked me via email [11]: "Wont the frequency response of a CBT array exhibit massive comb filtering due to the numerous time arrivals you hear that originate from the multiple speakers?"

The quick answer here is that comb filtering always exists in the array's magnitude and phase response but if the number of sources is sufficiently large, the comb filtering is not a problem because it exists above the operating frequency range of the array.

The author investigated this question by plotting the raw un-equalized magnitude/phase response and stick-figure impulse response of the CBT array of Fig. 1 while reducing the number of points comprising the array.

The first figure of the set shows the simulated results with a sufficient number of points (113) to push the comb filtering above 20 kHz. Subsequent simulations reduce the number of points to demonstrate the effect on the responses. The response was simulated at an on-axis distance of 80" from the front of the array.

8.1. Simulated CBT Comb Filtering and Effective CBT Upper Operating Frequency Limit versus Number of Array Sources

The following five graphs show that the comb filtering increases dramatically as the number of points forming the array is decreased. Comb filtering is only evident at frequencies above where the center-to-center spacing of the drivers is roughly 1/2 wavelength. At lower frequencies there is absolutely no comb filtering. This critical upper frequency is essentially the same frequency where the CBT arrays coverage pattern goes chaotic and no longer maintains its well-defined shape.

The following five figures illustrate the tradeoff between smoothness of magnitude and phase response as the number of sources in the array are reduced.

The simulations all have an odd number of points or sources contained in the array so that a source is always located at the center of the array.

All the following simulations in this section were run at a distance of 80" (about 2 m) from the front of the array.

The simulations start with the array composed of 113 array sources which provides smooth magnitude and phase response up to 20 kHz, and then proceeds downward eliminating about half the sources in steps of two until the number of sources is reduced to seven. At each reduction of two, the upper operating limit decreases by an octave reaching a limit of only about 625 Hz when the number of points are reduced to seven.

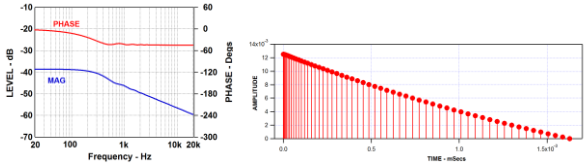

Fig. 27. Magnitude/phase responses (left) and stick-figure impulse response (right) with the array composed of 113 sources.

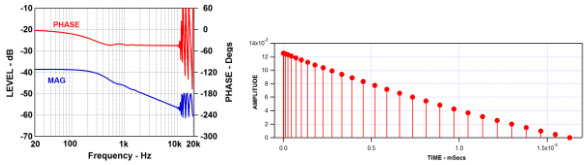

Fig. 28. Magnitude/phase responses (left) and stick-figure impulse response (right) with the array composed of 57 sources.

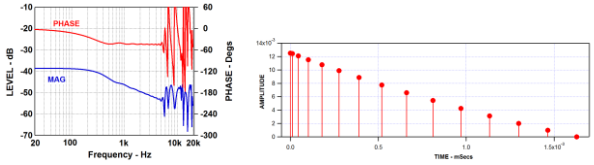

Fig. 29. Magnitude/phase responses (left) and stick-figure impulse response (right) with the array composed of 29 sources.

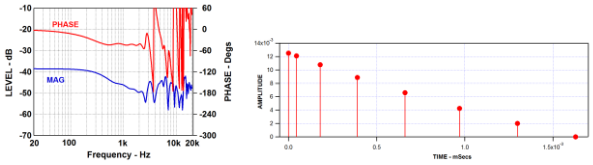

Fig. 30. Magnitude/phase responses (left) and stick-figure impulse response (right) with the array composed of 15 sources.

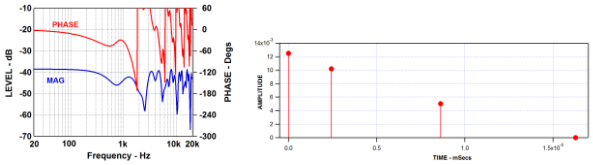

Fig. 31. Magnitude/phase responses (left) and stick-figure impulse response (right) with the array composed of only 7 sources.

8.2. Comb Filtering Observations

The figures indicate that the comb filtering dramatically decreases and the upper operating frequency range increases as sources are added to the array.

The point here is that there is always comb filtering in the magnitude and phase response of the CBT array (or any array for that matter), but if the number of points or sources that make up the array is high enough, the comb filtering only exists above the operating frequency range of the array.

9. EXPERIMENTAL MEASUREMENTS

Experimental measurements were accomplished on a small prototype 90 degree CBT circular-arc prototype ground-plane [7] line array. Magnitude/phase measurements were accomplished at various heights and angles in front of the array.

9.1. Test CBT Array

The following figure shows two views of the prototype array used to accomplish the experimental measurements. The array is about 23" tall, has a depth of 23", and uses 28 small headphone transducers.

The array is a one-way design and has a small-signal operating range of roughly 80 Hz to 16 kHz. The array maintains a vertical above-ground beamwidth of about 60° above 300 Hz. The array's center-to-center spacing of the headphone transducers is about 36 mm (1.42").

Fig. 32. The 90° ground-plane CBT test array which contains 28 small headphone transducers. The CBT Legendre shading is implemented with a five-bank network.

9.1.1. Test Array Shading

The test array has a five-bank shading network utilizing resistive attenuation with bank attenuation levels of 0, -2.5, -6, -9 and 12 dB. The shading network is shown in the following figure.

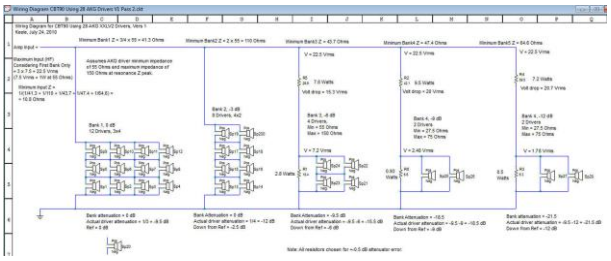

Fig. 33. The five-bank shading network that implements the Legendre shading for the test array.

9.1.2. Array Transducer

The array uses 28 each model XXL-V5 AKG headphone transducers. The driver has an OD of 30 mm with an 11.2 mm depth. The driver has a nominal impedance of 55 Ohms with a very-low free-air resonance of 110 Hz.

The following figure shows front and back views of the headphone driver along with the measured 2.83 Vrms/1m half-space frequency response.

Note the rising +3 dB on-axis response exhibited by the headphone transducer from about 150 Hz to 13 kHz! This rising response essentially fully compensates the power rolloff of the array! *QUERY NOTE: Does anyone*

reading this paper know how to implement this rising response characteristic in an arbitrary driver? If so they would make great CBT drivers!

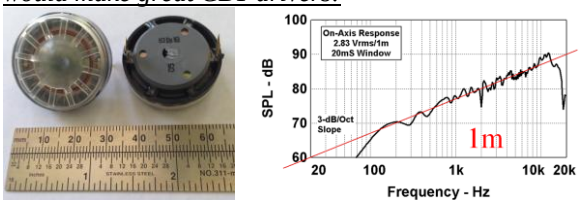

Fig. 34. Front and side views of the AKG XXL-V5 headphone transducer (left) along with a 2.83 Vrms/1m half-space response curve (right). Note rising +3 dB/octave response!

9.2. Test Setup and Location

The array was measured in my home theater listening room with a 7.5 ft ceiling and not in an anechoic environment. As a result of this live reflective test environment, the measurements exhibit some contamination from reflections from objects in the room and from the room's walls and ceiling. Windowing was used in the measurements to reduce reflections.

9.2.1. Multi-Mic Test Jig

In order to facilitate making response measurements at different heights in front of the test array, the author fabricated a multi-mic eight-position test jig to locate the test mic at various heights above the floor. The jig was formed of eight sets of mic clips, goosenecks, and mic flanges attached to a 1" x 2" wood strip. This mic test jig is shown in the next figure.

Fig. 35. Multi-mic test jig: plans (left), photo (right). This contraption when attached to a mic stand allows quick movement of the test mic to be positioned at different heights.

9.2.2. Test Environment

The next figure shows two views of tests being run in my listening room with the multi-mic test jig in place. The test jig was attached to the mic stand with Velcro straps. A ½" thick piece of blue Polystyrene insulation board was placed over the rug to form a reflective ground-plane barrier for the measurements.

Fig. 36. Two views of the listening room test environment with the test mic located 0.5 m high in the multi-mic test jig located in front of the array.

9.3. Measurement Test Gear, Software, and Test Conditions

All measurements were made with Dayton Audio's OmniMicV2 measurement system (http://www.parts-express.com/dayton-audio-omnimic-v2-computer-based-precision-room-measurement-system--390-792).

All curves were 1/12th octave smoothed. Windowing was set to blended with a 5 ms window, using a log sine wave sweep. All the phase curves generated by the OmniMic system are referenced to the peak of the impulse response and thus essentially automatically subtracts out the transport delay between the speaker and the test mic.

Special credit goes to Bill Waslo, developer of OmniMic, for programming a special version of OmniMic for me that allows response plots to be plotted with the standard aspect ratio of 25 dB/decade.

9.4. Magnitude-Phase Measurements

Several magnitude/phase measurements were accomplished at various heights and angles in front of and to the side of the test array of Fig. 32.

All measurements were accomplished at a distance of 0.5 m from the base of the array. Six magnitude/phase measurements were run at heights from 0.25 to 1.5 m in increments of 0.25 m.

With the exception of the first measurement, all magnitude measurements were approximately equalized flat using a minimum-phase digital processor: the MiniDSP 2x4 digital processing box from MiniDSP: http://www.minidsp.com/products/minidsp-in-a-box/minidsp-2x4.

9.4.1. Measurement with No Equalization

One un-equalized measurement was accomplished at a distance of 0.5 m in front of the base at a height of 0.25 m. This data is shown in the next figure. Note that even though no equalization is used, the array's magnitude and phase response is fairly flat and quite well behaved.

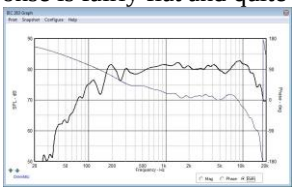

Fig. 37. Magnitude/phase response of the un-equalized array. The test mic was located at 0.5 m from base of the array at a height of 0.25 m.

9.4.2. Measurements with Equalization

All the following curves were taken with the system roughly equalized flat, over a frequency range of 80 Hz to 14 kHz, at 0.5 m from the array's base at a height of 0.25 m.

Measurements at Different Heights

All the vertical height measurements were accomplished at a distance of 0.5 m from the base of the array. Six magnitude/phase measurements were run at heights from 0.25 to 1.5 m in increments of 0.25 m. These measurements are shown in the next three figures.

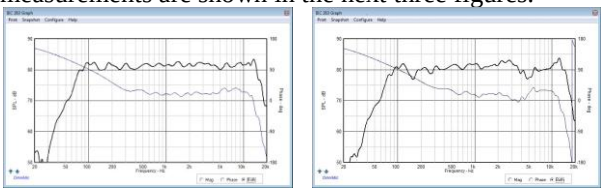

Fig. 38. Magnitude/phase responses of the equalized array at heights of 0.25 and 0.5 m high at a distance of 0.5 m from the base of the array.

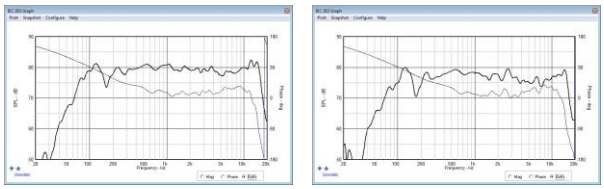

Fig. 39. Magnitude/phase responses of the equalized array at heights of 0.75 and 1.0 m high at a distance of 0.5 m from the base of the array.

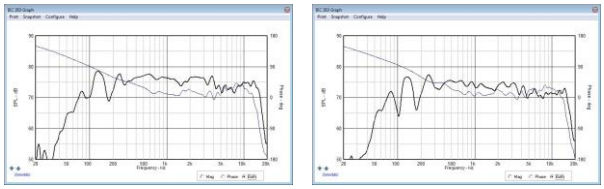

Fig. 40. Magnitude/phase responses of the equalized array at heights of 1.25 and 1.5 m high at a distance of 0.5 m from the base of the array.

Measurement at 45° Off-Axis Horizontal

A single measurement was made at 45° off-axis horizontal at a height of 0.25 m and 0.5 m from the base of the array. This measurement is shown in the next figure. Rotation was about the center of the front of the array. Note the uniformity of the curves even at 45° off axis!

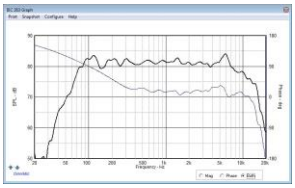

Fig. 41. Magnitude/phase response of the equalized array at a height of 0.25 m and 45° off-axis horizontal at a distance of 0.5 m from the base of the array.

9.4.3. Magnitude-Phase Measurement Observations

All these magnitude/phase curves are quite well behaved and similar to each other. These measurements show that when the line array's response is equalized magnitude/phase flat at a specific location in front of the array, it essentially remains magnitude/phase flat and minimum phase (near linear phase) at all the other locations as well! These other locations include points very close and far from the array, as well as point's off-axis vertical and horizontal.

9.5. Square Wave Response

The following measurements show the square wave response of the array of Fig. 32 at frequencies of 250 and 500 Hz. Heights of 0.25, 0.5, 0.75, and 1.0 m were measured at a distance of 0.5 m in front of the arrays base. One 45° off-axis horizontal measurement was taken at a height of 0.25 m and a distance of 0.5 m. The OmniMic oscilloscope function was used for these measurements with the generator set to square wave.

The square wave responses illustrate the direction and distance independent characteristics of the CBT's radiation. This means that the array is essentially time-aligned and thus will reproduce square waves at all these diverse locations!

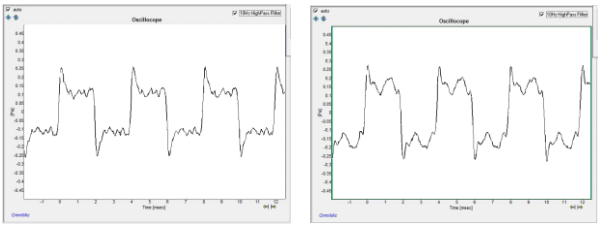

Fig. 42. Square wave response at 250 Hz at heights of 0.25 (left) and 0.5 m (right) at a distance of 0.5 m in front of the test array.

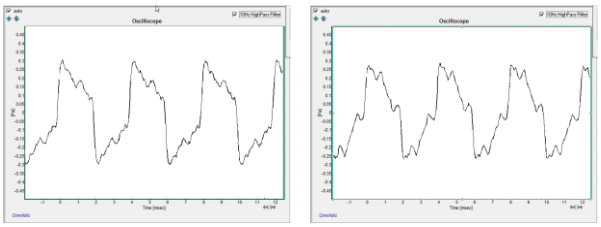

Fig. 43. Square wave response at 250 Hz at heights of 0.75 (left) and 1.0 m (right) at a distance of 0.5 m in front of the test array.

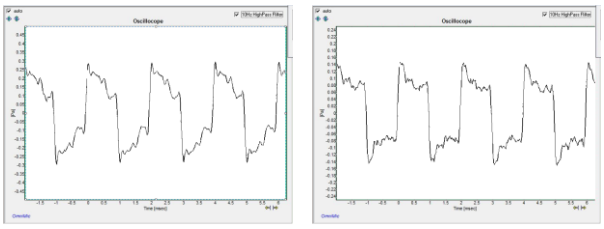

Fig. 44. Square wave response at 500 Hz at heights of 0.25 (left) and 0.5 m (right) at a distance of 0.5 m in front of the test array.

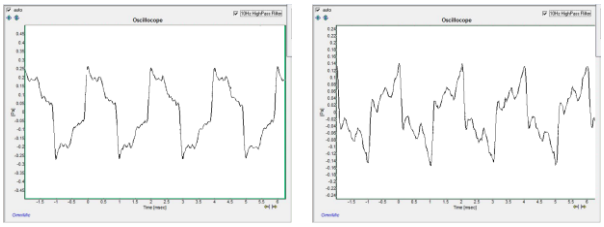

Fig. 45. Square wave response at 500 Hz at heights of 0.75 (left) and 1.0 m (right) at a distance of 0.5 m in front of the test array.

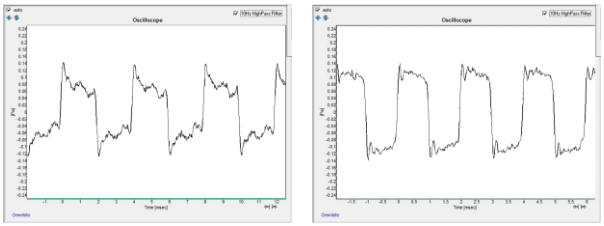

Fig. 46. Square wave response at 250 Hz (left) and 500 Hz (right) at a height of 0.25 m at 45° off-axis horizontal in front of the test array.

9.5.1. Square Wave Measurement Observations

Although these square wave responses are not perfect and exhibit many warts they clearly indicate that the CBT array is capability of reproducing square waves at many different locations. Repeating these measurements in a true anechoic reflection-free environment would probably greatly improve the measured square wave response.

10. SIMULATION SOFTWARE

Igor Pro 6 was used to run all the simulations in this paper http://www.wavemetrics.com/.

11. CONCLUSIONS

This paper explored the time and phase response of circular-arc CBT arrays through simulation and measurement. The paper showed that although the impulse response of the CBT array is spread out in time, it's phase response was found to be minimum phase at most locations within the array's coverage area.

When the magnitude response was equalized flat with a minimum-phase filter, the resultant phase was substantially linear phase over a broad frequency range. The phase linearity permitted the array to reproduce

square waves accurately at many different locations. Accurate loudspeaker square wave reproduction may not be important to people in the pro-sound industry but it is quite important to others, particularly in the high-end loudspeaker industry.

Calculated sound fields for the CBT array showed that the radiation of the array essentially mimics a point source but with the controlled coverage of the CBT array's radiation. The response of the array was found to be essentially time aligned with a radiation that was found to originate at the center of curvature of the circular-arc array.

Several simulations of magnitude/phase and impulse response illustrated that comb filtering is minimized along as the number of sources in the array is high enough to shove the comb filtering above the upper operating frequency limit of the array.

Calculations of stick-figure impulse response showed that the CBT array's impulse response resembles a shape that looks like a laterally-viewed roller coaster track.

12. ACKNOWLEDGEMENTS

This work was supported solely by the author!

13. REFERENCES

[1] P. H. Rogers, and A. L. Van Buren, "New Approach to a Constant Beamwidth Transducer," J. Acous. Soc. Am., vol. 64, no. 1, pp. 38-43 (1978 July).

[2] A. L. Van Buren, L. D. Luker, M. D. Jevnager, and A. C. Tims, "Experimental Constant Beamwidth Transducer," J. Acous. Soc. Am., vol. 73, no. 6, pp. 2200-2209 (1983 June).

[3] D. B. Keele, Jr., "The Application of Broadband Constant Beamwidth Transducer (CBT) Theory to Loudspeaker Arrays," 109th Convention of the Audio Engineering Society, Preprint 5216 (Sept. 2000).

[4] D. B. Keele, Jr., "Implementation of Straight-Line and Flat-Panel Constant Beamwidth Transducer (CBT) Loudspeaker Arrays Using Signal Delays," 113th Convention of the Audio Engineering Society, Convention paper 5653 (Oct. 2002).

[5] D. B. Keele, Jr., "The Full-Sphere Sound Field of Constant Beamwidth Transducer (CBT) Loudspeaker Line Arrays," J. Aud. Eng. Soc., vol. 51, no. 7/8., pp. 611-624 (July/August 2003).

[6] D. B. Keele, Jr., "Practical Implementation of Constant Beamwidth Transducer (CBT) Loudspeaker Circular-Arc Line Arrays," presented at the 115th Convention of the Audio Engineering Society, New York, Convention paper 5863 (Oct. 2003).

[7] D. B. Keele, Jr., D. J. Button, "Ground-Plane Constant Beamwidth Transducer (CBT) Loudspeaker Circular-Arc Line Arrays," presented at the 119th Convention of the Audio Engineering Society, New York (Oct. 2005).

[8] D. B. Keele, Jr., "A Performance Ranking of Seven Different Types of Loudspeaker Line Arrays," presented at the 129th Convention of the Audio Engineering Society, San Francisco (Nov. 2010).

[9] D. B. Keele, Jr., "Implementation of Segmented Circular-Arc Loudspeaker Arrays," presented at the 139th Convention of the Audio Engineering Society, New York (Oct.-Nov. 2015).

[10] X. Feng, Y. Shen, D. B. Keele, Jr., and J. Xia, "Directivity-Customizable Loudspeaker Arrays Using Constant-Beamwidth Transducer (CBT) Overlapped Shading," presented at the 139th Convention of the Audio Engineering Society, New York (Oct.-Nov. 2015).

[11] Private email between the author and George Louis (www.AbsolutePolarity.com) related to the possible comb filtering caused by the CBT array's multiple sources.